ChemComm

COMMUNICATION

View Article Online
View Journal | View Issue

Cite this: *Chem. Commun.*, 2026, **62**, 7519

Received 4th February 2026,
Accepted 7th March 2026

DOI: 10.1039/d6cc00736h

rsc.li/chemcomm

Catalyst-free insertion of carbon monoxide into terminal Mg–C(sp^3) bonds

M. Kubisz,[a] I. Fernandez *[b] and T. J. Hadlington *[a]

We describe the catalyst-free Insertion of carbon monoxide (CO) into magnesium alkyl bonds, leading exclusively to enediolate compounds through C–C coupling. Computational investigations suggest a metallated ketene intermedate. Ultimately, the formed enedoliate fragment can be liberated on reaction with a silane, establishing a potential pathway for s-block metal alkyl formylation catalysis.

The functionalization of carbon monoxide (CO) as an abundant C1 building block forms the foundation of numerous industrially significant catalytic processes,[1] such as hydroformylation,[2–4] the Fischer–Tropsch process,[5–7] and the Pauson–Khand reaction.[8,9] These processes are reliant on transition metal catalysts, perhaps the most prominent example being the cobalt and ruthenium catalysts required for alkene hydroformylation. Contemporary chemistry looks towards displacing these often high-cost, toxic systems with more sustainable derivatives.[10,11] As such, recent efforts have explored the utility of main group elements in CO valorisation, demonstrating numerous stoichiometric transformations such as reductive CO coupling, complete C–O bond scission, and M–H insertion.[12,13] In this space, the alkaline earth metals have been notably prolific.[14]

In landmark simultaneous reports, the groups of Hill and Jones demonstrated that magnesium hydride systems readily insert CO into their Mg–H bonds, leading to dimerization in forming ethylene diolate complexes (Fig. 1(a)),[15,16] and can catalytically silylate CO to methanol equivalents.[16] This was later extended to calcium and insertion into M–N bonds (M = Mg, Ca) in formal CO reductive amination,[17] to Ba,[18] and by our group to Be.[19] The Jones group has also demonstrated numerous examples of reductive CO homologation using Mg^I dimers, leading to *e.g.* the ethenediolate, deltate and benzenehexolate anions.[20,21] More recently, CO activation has been extended to anionic alkaline earth metal(I) dimers[22,23] and hydride complexes.[24] These promising transformations demonstrate the utility of these abundant metals in functionalising CO. Yet, catalyst-free alkaline earth-mediated transfer of this C1 building block to hydrocarbon functional groups is limited, stymying progress in displacing transition metals in hydroformylation catalyses. Early work here demonstrated that Grignard reagents react with a CO atmosphere in the presence of $Ni(CO)_4$,[25] or simply with an excess of $Ni(CO)_4$ leading to a range of CO-functionalised products, including acyloins *via* CO coupling (Fig. 1(b)).[26] In 2025, Maron, Xu, and co-workers extended this chemistry to well-defined ^{Dip}Nacnac-stabilised magnesium alkyl species (^{Dip}Nacnac = $[HC\{C(Me)Ndip\}_2]^-$, Dip = 2,6-^{i}Pr$_2$C$_6$H$_3$), leading to alkyl-substituted diolate and triolate complexes through Ni-catalysed cabonylation (Fig. 1(c)).[27] To date, only highly

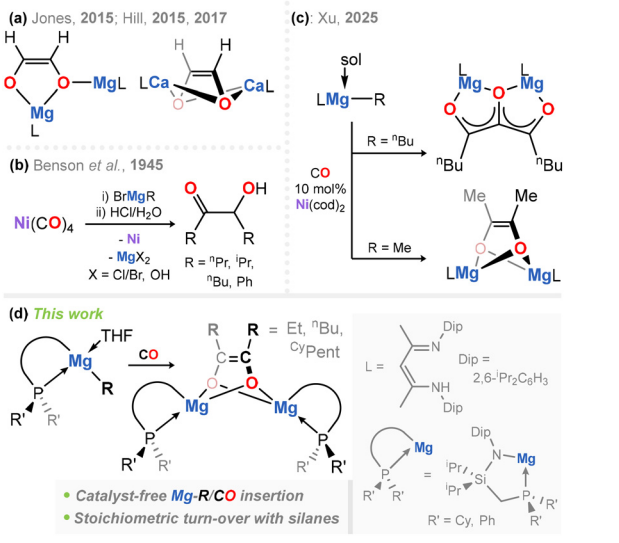

Fig. 1 (a): initial examples of CO reactivity with alkaline earth hydrides; (b): early reports on the Ni-aided reactivity of CO with magnesium organyls; (c): recently reported Ni-catalysed CO insertion in Mg–C bonds; (d): *this work* – catalyst-free insertion of CO into Mg–C(sp^3) bonds.

[a] *Fakultät für Chemie, Technische Universität München, Lichtenberg Strasse 4, 85747, Garching, Germany. E-mail: terrance.hadlington@tum.de*
[b] *Departamento de Química Orgánica I and Centro de Innovación en Química Avanzada, Facultad de Ciencias Químicas, Universidad Complutense de Madrid, 28040, Madrid, Spain. E-mail: israel@quim.ucm.es*

strained[28] and/or activated Mg–C bonds are known to insert CO without need for a catalyst,[29] with occurrences being very rare indeed, whilst Harder and co-workers reported a unique reactive pathway involving 1,1-addition of CO into intramolecular Mg-benzyl fragments.[30]

In this work (Fig. 1(d)), we report the facile insertion of carbon monoxide into the Mg–C bonds of terminal magnesium alkyl complexes, in the absence of a catalyst. This exclusively leads to alkyl-functionalised ethene diolate products, with no significant formation of side-products. We additionally demonstrate that these species undergo reaction with phenyl silane, in the formation of the corresponding magnesium hydride complex. Computational assessment of the reaction coordinate suggests a divergent mechanism to that observed in hydride insertion, forming a ketenyl intermediate prior to formation of the target products. These results move a step closer to achieving transition metal-free alkene carbonylation processes.

This work began with the synthesis of magnesium organyl complexes bearing our developed phosphine-appended amido ligands (*viz.* ^{R}L; ^{R}L = {[$R_2PCH_2Si(^{i}Pr)_2$](Dip)N}; Dip = 2,6-$^{i}Pr_2C_6H_3$; R = Ph, Cy), akin to reported beryllium hydride chemistry.[19] This utilized two approaches: (i) the protonated ligands are reacted with $^{n}Bu_2Mg$, in loss of butane and formation of ^{R}LMg(^{n}Bu), or (ii) the ligand potassium salts are reacted with Grignard reagents (*i.e.* RMgBr), in loss of KBr and formation of the target compounds (Scheme 1). This led to five complexes featuring the ^{Cy}L ligand (R = Me, ^{n}Bu, Et, ^{Cy}Pent, and Ph), and a single complex featuring the ^{Ph}L ligand (R = ^{n}Bu; Scheme 1).† Solid-state structures of complexes bearing Et (**1-Cy**), ^{n}Bu (**2-Cy** and **-Ph**), and ^{Cy}Pent (**3-Cy**) groups, crystallise as 4-coordinate monomeric THF adducts (*e.g.* **2-Ph**, Fig. 2(a)), whilst Me and Ph complexes (**4-Cy** and **5-Cy**, respectively) are isolated as THF-free dimeric species, bridged by their organyl groups. The range of P–Mg bond lengths (2.533–2.985 Å) lies within those of the relatively few phosphine-coordinated magnesium complexes reported.[31–39] The shortest Mg–C distance of 2.130(6) Å, observed in **2-Cy**, aligns with those in established monomeric magnesium alkyl species,[40–42] as do those observed in dimeric **4-Cy** and **5-Cy**, which are somewhat longer (*e.g.* 2.654(1) Å in **4-Cy**). The $^{31}P\{^{1}H\}$ NMR spectra display a singlet resonance for all compounds with shifts similar to those for ^{R}LK salts.[43,44] Alkyl ligands are clearly observed in the ^{1}H NMR spectra – notable high-field shifts are observed for the α-carbon of such species (*e.g.* **2-Cy**: −0.09 ppm).

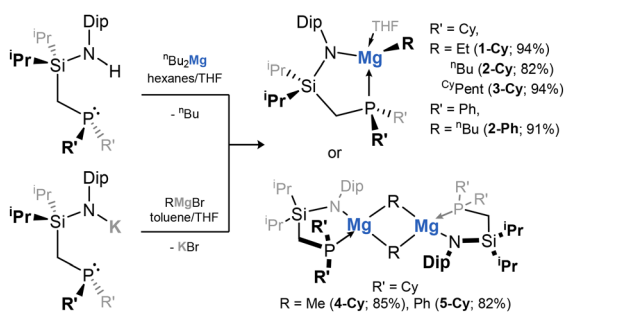

Scheme 1 Synthesis of Mg-organyl compounds **1–5** (yields in parentheses).

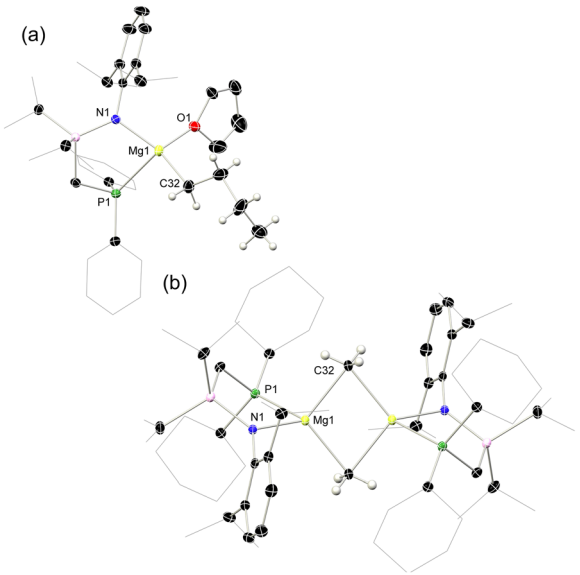

Fig. 2 Molecular structures of (a) **2-Ph**, and (b) **4-Cy**, with thermal ellipsoids at 30% probability and hydrogen atoms removed for clarity aside from those of the Mg-alkyl groups. Selected bond lengths (Å) and angles (°) in **2-Ph**: Mg1-P1 2.6969(7); Mg1-O1 2.065(1); Mg1-C32 2.174(3); Mg1-N1 2.035(1); N1-Mg1-P1 82.77(4). In **4-Cy**: Mg1-P1 2.654(1) Mg1-N1 2.018(1); Mg1-C32 2.243(2); Mg1-C32′ 2.277(2); Mg1···Mg1′ 2.787(1); N1-Mg1-P1 86.62(4); Mg1-C32-Mg1′ 76.13(5); C32-Mg1-C32′ 103.87(6).

Following isolation of the above magnesium organyls, their reactivity towards CO was investigated. Samples of ^{n}Bu substituted **2-Cy** or **2-Ph** as solutions in C_6D_6 show a clear reaction with CO over the course of two days, in a Teflon-sealed NMR tube charged at atmospheric pressure. In addition to being sluggish, *in situ* $^{31}P\{^{1}H\}$ NMR analyses were indicative of the formation of multiple products. To improve these points, the reactions were repeated on a preparative scale in a Teflon-sealed Schlenk flask (*e.g.* 200 mg) or Fischer Porter bottle (*e.g.* up to 1.8 g), with rapid stirring and 2 bar CO pressure.‡ After 24 h, NMR spectroscopic analysis indicates complete conversion of all starting material, and now formation of a single new species. ^{1}H NMR spectra indicate a shift of the alkyl α-carbon C–H resonance away from those observed at −0.09 (**2-Cy**) and 0.20 (**2-Ph**) ppm, giving initial evidence for insertion into the Mg–C bonds in these species. Concentrated pentane solutions of these products stored at −30 °C overnight yield large colourless crystals – single-crystal X-ray diffraction (SC-XRD) analysis reveals these to be dimagnesium dec-5-enediolate complexes **6-Cy** and **6-Ph** (Fig. 3(a) and (b)), isolated in relatively low yields of 38 and 28% due to their high solubility. As observed in reported magnesium hydride chemistry, these species likely arise from initial insertion of CO into Mg–C^{Bu} bonds, followed by C–C coupling (*vide infra*). Importantly, this forms a new C10 chain through combining two C4 chains and two C1 building blocks, without an external catalyst or significantly activated Mg–C bonds. Importantly, such reactivity of metal-alkyls is only known for early transition metal systems (*e.g.* Zr, Hf),[45–47] and

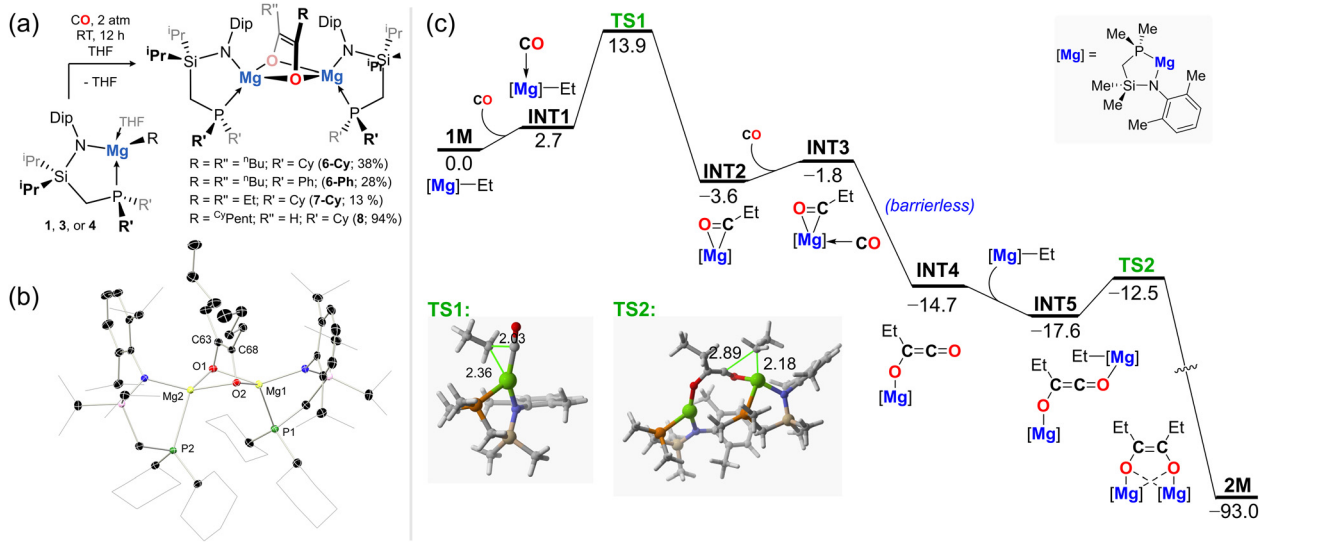

Fig. 3 (a) Synthesis of magnesium enediolate compounds **6–8** through reaction of magnesium alkyls with carbon monoxide, with compound numbers and isolated yields in parentheses; (b) Molecular structure of **6-Cy**, with thermal ellipsoids at 30% probability and hydrogen atoms removed for clarity. Selected bond lengths (Å) and angles (°): C63-C68 1.362(2); O1-C63 1.406(2); O2-C68 1.407(2); Mg1-O1 2.052(1); Mg1-O2 2.054(1); Mg2-O1 2.037(1); Mg2-O2 2.057(1); Mg1-P1 2.6763(8); P2-Mg2 2.6322(7); (c) Computed reaction profile for the transformation of **1M** in the presence of CO. Relative free energies (DG, at 298 K) and bond distances are given in kcal/mol and angstroms, respectively. All data have been computed at the (CPMD)-RI-BP86-D3BJ/def2-TZVPP//(CPCM)-RI-BP86-D3BJ/def2-SVP level.

lanthanide derivatives.[48] Structurally, a clear C=C bond is found between C63 and C68 in the dec-5-ene chain (d = 1.362(2) Å), akin to distances observed in reported ethenediolate ligands. The $^{13}C\{^1H\}$ NMR spectra for both compounds are in keeping with this ligand motif: resonances relating to alkenyl-C centres are observed at δ = 139.7 (**6-Cy**) and 140.4 (**6-Ph**) ppm, with the α-C of the ^{n}Bu chain observed at 34.5 (**6-Cy**) and 30.3 (**6-Ph**) ppm. A single ligand environment is observed for the two ^{R}L ligands, *e.g.* with a single resonance observed in their $^{31}P\{^1H\}$ NMR spectra (δ = −14.7 (**6-Cy**) and −23.6 (**6-Ph**) ppm), reflecting the solid-state structure of these species, whereby their phosphine chelating arms lie *trans* to the ethenyl unit (see Fig. 3(b)).

Interestingly, this observed reactivity is divergent from recently reported Ni-catalysed insertion of CO into the Mg–C^{Bu} bond of [^{Dip}NacnacMgBu·(OEt$_2$)], whereby three equiv. of CO react per two Mg centres, forming the unique $[Bu_3C_3O_3]^{-2}$ anion.[27] Small R groups (*e.g.* Me) were found react akin to the above-described **2-Cy** and **2-Ph**. As such, we extended our reactivity studies to **1** and **3–5**, to explore any differences. We are surprised to find that dimeric Me and Ph complexes (*i.e.* **4-Cy** and **5-Cy**) in THF solutions do not react with CO, even after prolonged reaction times with heating, potentially due to their dimeric nature quenching reactivity. In contrast, monomeric Et and ^{Cy}Pent species **1-Cy** and **3-Cy** demonstrate clean reactivity towards CO (2 atm, RT), forming single species after 24 h. NMR spectroscopic data for the former is in keeping with that for **6-Cy**, indicative of the formation of novel hex-3-enediolate magnesium complex, **7-Cy** (Fig. 3(a)). In contrast, *in situ* ^{1}H NMR spectra for reactions with **3-Cy** indicate the elimination of one equiv. cyclopentene per two Mg centres, and the presence of two new ligand environments ($^{31}P\{^1H\}$ NMR: δ = −13.6 and −14.2 ppm). As per complexes **6** and **7**, ^{13}C NMR indicates the presence of a now unsymmetrical enediolate moiety (δ = 127.0, O*C*-H; 139.1, O*C*-^{Cy}Pent ppm), whilst a new 1H singlet is observed at δ = 6.07 ppm in the ^{1}H NMR which aligns with resonances for known ethenediolate C–*H* moieties (*e.g.* in Mg and Ca complexes in Fig. 1(a): 5.63 and 5.00 ppm, respectively), and in Xu's but-3-enediolate.[15,17,27] Thus, reaction of ^{Cy}Pent compound **3-Cy** with CO leads to the 2-cyclopentyl-ethenedoliate complex **8-Cy** (Fig. 3(a)). This, again, is divergent from the reported Ni-catalysed reaction between [^{Dip}NacnacMg(^{Cy}Pent)·(THF)] and CO, which rather leads to a methylenecyclopentane species through an intermediary 1,2-hydride shift. These observations highlight the effect of small changes in ligand on the course of a reaction in reactive CO chemistry, and indeed the effect of a catalytic transition metal on affecting the reaction coordinate.

Given the unique nature of the reaction between CO and the described magnesium alkyl complex, the mechanism for this process was investigated computationally by means of Density Functional Theory (DFT) calculations (see SI for details). As depicted in Fig. 3(b), the process begins with the slightly endergonic (ΔG = 2.7 kcal mol^{-1}) coordination of CO to the magnesium center to produce **INT1**. From this species, insertion of the coordinated CO into the Mg–C^{Et} bond takes place to produce the k^2-C,O-propionyl complex **INT2** in an exergonic process (ΔG = −3.6 kcal mol^{-1}). This insertion reaction requires a low free activation barrier of 13.9 kcal mol^{-1} (from the separate reactants **1M** and CO) *via* **TS1**, a saddle point associated with the formation of the new C–C bond with concomitant Mg-C^{Et} bond rupture. Coordination of a second molecule of CO leads to slightly endergonic (ΔG = 1.8 kcal mol^{-1}) formation of intermediate **INT3**, from which a new, strongly exergonic (ΔG = −12.9 kcal mol^{-1}) and barrierless insertion reaction takes place to produce the ketene intermediate **INT4** (see SI, Fig. S91).

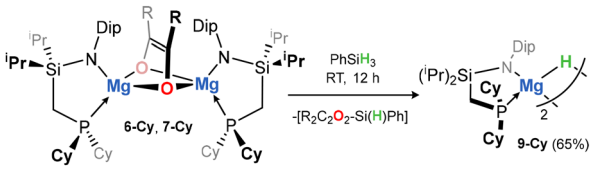

Scheme 2 The reaction of complex **6-Cy** with phenyl silane, forming magnesium hydride compound **9** (isolated yield in parentheses).

Once **INT4** is formed, exergonic coordination of its ketene carbonyl group to a new molecule of **1M** would lead to **INT5**, from which the final ethenediolate species **2M** can be formed. This final, highly exergonic reaction (ΔG = −75.4 kcal mol^{-1}) takes place *via* **TS2** with a rather low free activation barrier of only $\Delta G^{\neq}$ = 5.1 kcal mol^{-1}, which is fully consistent with a kinetically accessible process occurring at room temperature.

Finally, having observed the (catalyst-free) insertion of CO into Mg–C bonds, we sought to liberate the organic fragment in service of a magnesium-centred catalytic process akin to hydroformylation. No reaction is observed between complexes **6**, **7**, and **8** and dihydrogen (up to 2 bar, 70 °C). Reaction with a hydridic reagent, however, is more promising: addition of $PhSiH_3$ to C_6D_6 solutions of **6-Cy** leads to the slow formation of a new species (Scheme 2), with a clear triplet resonance observed in the ^{1}H NMR spectrum at δ = 3.98 ppm – we attribute this to a dimeric Mg–H system, whereby the hydride ligand couples to two Cy_2P-groups of the ligand scaffold. Storage of such samples overnight at ambient temperature leads to the formation of large colourless crystals. These are found to be hydride complex **9** (Fig. 4), formed through metathesis of Mg–O bonds in **6-Cy**. Compound **9** is a relatively rare example of a phosphine-coordinated group 2 hydride complex, with previous examples being reported by Harder and co-workers.[35,37] The Mg···Mg distance of 2.795(1) Å is similar to those observed in reported dimeric magnesium hydride complexes. The P-Mg distance is significantly contracted when compared with all other species reported here, at 2.556(1) Å, presumably due to the low-coordinate Mg centres in the absence of alkyl C–H···Mg stabilisation. We are surprised to find, in spite of this, that **9** does not readily coordinate THF, and seems to exclusively crystallise as the solvent-free dimer. This is in contrast to Nacnac-stabilised derivatives, whose reactivity in the solvent-free state is significantly amplified. This may suggest a high reactivity of group 2 complexes stabilised by our phosphine-appended ligand systems, *e.g.* ^{R}L, which we will report in due course.

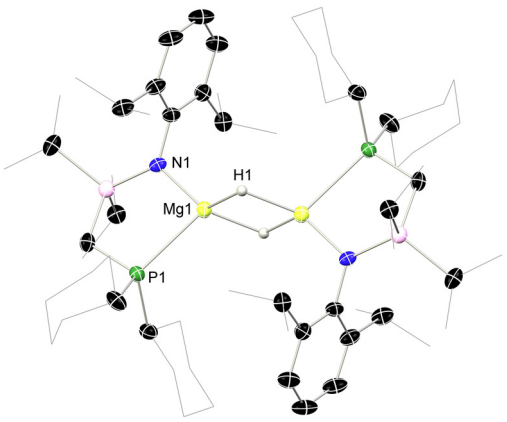

Fig. 4 Molecular structure of **9**, with thermal ellipsoids at 30% probability and hydrogen atoms removed for clarity. Selected bond lengths (Å) and angles (°): Mg1-P1 2.556(1); Mg1-N1 2.055(4); Mg1-H1 1.85(3); Mg1-H1′ 1.86(2); Mg1···Mg1′ 2.795(1); N1-Mg1-P1 90.9(1).

MK: investigation, formalanalysis, data curation, writing – review and editing. IF: methodology (computational), formal analysis (computational), funding acquisition, writing – original draft and review and editing. TJH: conceptualisation, supervision, funding acquisition, project administration, writing – original draft.

Conflicts of interest

There are no conflicts to declare.

Data availability

The data supporting this article have been included as part of the supplementary information (SI). Supplementary information is available. See DOI: https://doi.org/10.1039/d6cc00736h.

CCDC 2528198–2528207 contain the supplementary crystallographic data for this paper.[49a–j]

Acknowledgements

T. J. H. thanks the ERC for a Starting grant (Project 101076897 – SINGAMBI), the DFG for funding (Project Nr. 523956566), and Prof. Thomas Fässler for his continued support. I. F. is grateful for financial support from the Spanish MICIU/AEI/10.13039/501100011033 (Grant PID2022-139318NB-I00).

References

† On one occasion, a few crystals of the Et_2Mg complex ^{Cy}LMgEt(μ-$MgEt_2$)EtMg^{Cy}L were found co-crystallised with **3**. These could not be separated, and as such clean analytical data for that complex could not be attained. Nevertheless, the X-ray crystal structure is given in the Supporting Information (Fig. S90).
‡ We presume that higher pressures promote more selective reactions due to the low solubility of CO in aliphatic solvents – that is, lower CO pressures perhaps lead to longer-lived intermediates, which undergo divergent reactivity.

1 *Carbon Monoxide in Organic Synthesis: Carbonylation Chemistry*, ed. B. Gabriele, Wiley, 1st edn, 2021.
2 A. Börner and R. Franke, *Hydroformylation: fundamentals, processes, and applications in organic synthesis*, Wiley-VCH Verlag GmbH & Co, Weinheim, 2016.
3 B. Zhang, D. Peña Fuentes and A. Börner, *ChemTexts*, 2022, **8**, 2.
4 R. Franke, D. Selent and A. Börner, *Chem. Rev.*, 2012, **112**, 5675–5732.
5 A. de Klerk, *Fischer-Tropsch refining*, Wiley-VCH Verlag & Co. KGaA, Weinheim, 2011.
6 K. T. Rommens and M. Saeys, *Chem. Rev.*, 2023, **123**, 5798–5858.
7 A. Yohannes and I. Gates, *Coord. Chem. Rev.*, 2026, **547**, 217096.
8 *The Pauson-Khand Reaction: Scope, Variations and Applications*, ed., R. Rios Torres, Wiley, 1st edn, 2012.

9 A. Lledó and J. Solà, *Adv. Synth. Catal.*, 2024, **366**, 574–592.
10 R. Luque and F. Leung-Yuk Lam, *Sustainable Catalysis: Energy-Efficient Reactions and Applications*, Wiley, 1st edn, 2018.
11 K. M. P. Wheelhouse, R. L. Webster and G. L. Beutner, *Org. Process Res. Dev.*, 2023, **27**, 1157–1159.
12 S. Fujimori and S. Inoue, *J. Am. Chem. Soc.*, 2022, **144**, 2034–2050.
13 D. W. Stephan, *Chem. Soc. Rev.*, 2023, **52**, 4632–4643.
14 M. J. Evans and C. Jones, *Chem. Soc. Rev.*, 2024, **53**, 5054–5082.
15 R. Lalrempuia, C. E. Kefalidis, S. J. Bonyhady, B. Schwarze, L. Maron, A. Stasch and C. Jones, *J. Am. Chem. Soc.*, 2015, **137**, 8944–8947.
16 M. D. Anker, M. S. Hill, J. P. Lowe and M. F. Mahon, *Angew. Chem., Int. Ed.*, 2015, **54**, 10009–10011.
17 M. D. Anker, C. E. Kefalidis, Y. Yang, J. Fang, M. S. Hill, M. F. Mahon and L. Maron, *J. Am. Chem. Soc.*, 2017, **139**, 10036–10054.
18 X. Shi, C. Hou, C. Zhou, Y. Song and J. Cheng, *Angew. Chem., Int. Ed.*, 2017, **56**, 16650–16653.
19 T. J. Hadlington and T. Szilvási, *Nat. Commun.*, 2022, **13**, 461.
20 K. Yuvaraj, I. Douair, A. Paparo, L. Maron and C. Jones, *J. Am. Chem. Soc.*, 2019, **141**, 8764–8768.
21 A. Paparo, K. Yuvaraj, A. J. R. Matthews, I. Douair, L. Maron and C. Jones, *Angew. Chem., Int. Ed.*, 2021, **60**, 630–634.
22 H.-Y. Liu, R. J. Schwamm, S. E. Neale, M. S. Hill, C. L. McMullin and M. F. Mahon, *J. Am. Chem. Soc.*, 2021, **143**, 17851–17856.
23 D. T. Nguyen, R. Mondal, M. J. Evans, J. M. Parr and C. Jones, *Angew. Chem., Int. Ed.*, 2025, **64**, e202500264.
24 J. S. McMullen, R. Huo, P. Vasko, A. J. Edwards and J. Hicks, *Angew. Chem., Int. Ed.*, 2023, **62**, e202215218.
25 W. L. Gilliland and A. A. Blanchard, *J. Am. Chem. Soc.*, 1926, **48**, 410–420.
26 F. L. Benton, M. C. Voss and P. A. McCusker, *J. Am. Chem. Soc.*, 1945, **67**, 82–83.
27 M. Wang, Y. Cai, T. Rajeshkumar, L. Maron and X. Xu, *Chem. – Eur. J.*, 2025, **31**, e202404594.
28 K. Yuvaraj and C. Jones, *Chem. Commun.*, 2021, **57**, 9224–9227.
29 A. J. Boutland, A. Carroll, C. Alvarez Lamsfus, A. Stasch, L. Maron and C. Jones, *J. Am. Chem. Soc.*, 2017, **139**, 18190–18193.
30 O. P. E. Townrow, T. Richter, J. Langer and S. Harder, *Chem. – Eur. J.*, 2025, **31**, e202404028.
31 J. Pahl, T. E. Stennett, M. Volland, D. M. Guldi and S. Harder, *Chem. – Eur. J.*, 2019, **25**, 2025–2034.
32 A. Pape, M. Lutz and G. Müller, *Angew. Chem., Int. Ed. Engl.*, 1994, **33**, 2281–2284.
33 M. M. Meinholz, S. K. Pandey, S. M. Deuerlein and D. Stalke, *Dalton Trans.*, 2011, **40**, 1662.
34 N. D. Contrella and R. F. Jordan, *Organometallics*, 2014, **33**, 7199–7208.
35 J. Langer, I. Kosygin, R. Puchta, J. Pahl and S. Harder, *Chem. – Eur. J.*, 2016, **22**, 17425–17435.
36 A. Koch, S. Krieck, H. Görls and M. Westerhausen, *Inorganics*, 2016, **4**, 39.
37 J. Langer, B. Maitland, S. Grams, A. Ciucka, J. Pahl, H. Elsen and S. Harder, *Angew. Chem., Int. Ed.*, 2017, **56**, 5021–5025.
38 S. Bestgen, C. Schoo, B. L. Neumeier, T. J. Feuerstein, C. Zovko, R. Köppe, C. Feldmann and P. W. Roesky, *Angew. Chem., Int. Ed.*, 2018, **57**, 14265–14269.
39 L. Garcia, M. D. Anker, M. F. Mahon, L. Maron and M. S. Hill, *Dalton Trans.*, 2018, **47**, 12684–12693.
40 J. Spielmann, D. F.-J. Piesik and S. Harder, *Chem. – Eur. J.*, 2010, **16**, 8307–8318.
41 M. H. Chisholm, K. Choojun, A. S. Chow, G. Fraenkel and J. C. Gallucci, *Inorg. Chem.*, 2013, **52**, 11302–11310.
42 M. S. Hill, D. J. MacDougall and M. F. Mahon, *Dalton Trans.*, 2010, **39**, 11129.
43 P. M. Keil, T. Szilvási and T. J. Hadlington, *Chem. Sci.*, 2021, **12**, 5582–5590.
44 T. L. Kalkuhl, I. Fernández and T. J. Hadlington, *Chemistry*, 2025, **11**, 102349.
45 P. Hofmann, M. Frede, P. Stauffert, W. Lasser and U. Thewalt, *Angew. Chem., Int. Ed. Engl.*, 1985, **24**, 712–713.
46 G. Erker, P. Czisch, R. Schlund, K. Angermund and C. Krüger, *Angew. Chem., Int. Ed. Engl.*, 1986, **25**, 364–365.
47 L. P. Spencer and M. D. Fryzuk, *J. Organomet. Chem.*, 2005, **690**, 5788–5803.
48 M. R. Luevano, C. R. Stennett, J. W. Ziller and W. J. Evans, *J. Am. Chem. Soc.*, 2025, **147**(15), 12386–12391.
49 (*a*) CCDC 2528198: Experimental Crystal Structure Determination, 2026, DOI: 10.5517/ccdc.csd.cc2qvss5; (*b*) CCDC 2528199: Experimental Crystal Structure Determination, 2026, DOI: 10.5517/ccdc.csd.cc2qvst6; (*c*) CCDC 2528200: Experimental Crystal Structure Determination, 2026, DOI: 10.5517/ccdc.csd.cc2qvsv7; (*d*) CCDC 2528201: Experimental Crystal Structure Determination, 2026, DOI: 10.5517/ccdc.csd.cc2qvsw8; (*e*) CCDC 2528202: Experimental Crystal Structure Determination, 2026, DOI: 10.5517/ccdc.csd.cc2qvsx9; (*f*) CCDC 2528203: Experimental Crystal Structure Determination, 2026, DOI: 10.5517/ccdc.csd.cc2qvsyb; (*g*) CCDC 2528204: Experimental Crystal Structure Determination, 2026, DOI: 10.5517/ccdc.csd.cc2qvszc; (*h*) CCDC 2528205: Experimental Crystal Structure Determination, 2026, DOI: 10.5517/ccdc.csd.cc2qvt0f; (*i*) CCDC 2528206: Experimental Crystal Structure Determination, 2026, DOI: 10.5517/ccdc.csd.cc2qvt1g; (*j*) CCDC 2528207: Experimental Crystal Structure Determination, 2026, DOI: 10.5517/ccdc.csd.cc2qvt2h.